Energy 284 (2023) 128709

Contents lists available at ScienceDirect

Energy

journal homepage: www.elsevier.com/locate/energy

Life cycle assessment and cost benefit analysis of concentrated solar thermal gasification of biomass for continuous electricity generation

Yi Fang [a], Xian Li [b], Simon Ascher [a], Yize Li [a], Leilei Dai [c], Roger Ruan [c], Siming You [a,*]

[a] James Watt School of Engineering, University of Glasgow, Glasgow, G12 8QQ, UK
[b] Institute of High Performance Computing (IHPC), Agency for Science, Technology and Research (A*STAR), 1 Fusionopolis Way, #16-16 Connexis, Singapore 138632, Republic of Singapore
[c] Center for Biorefining and Department of Bioproducts and Biosystems Engineering, University of Minnesota, 1390 Eckles Ave., St. Paul, MN55108, USA

ARTICLE INFO

Handling Editor: Krzysztof (K.J.) Ptasinski

Keywords:
Biomass
Concentrated solar thermal
Gasification
Producer gas
Life cycle assessment
Cost benefit analysis
Sensitivity analysis

ABSTRACT

The hybridization of solar and biomass energy systems is a promising technology for mitigating the issues of energy generation-related greenhouse gas emissions and high energy prices. The global warming potential and economic feasibility of a hybrid solar-bioenergy system, comprised of a concentrated solar tower, biomass gasifier, thermal storage, and combined cycle gas turbine, have been evaluated by using life cycle assessment and cost benefit analysis, respectively. Sensitivity analysis is carried out to identify the hotspots of costs and emissions. The net present worth of the proposed system at the 30th year was calculated to be about €–0.7 billion. There are two suggestions to enhance the economic viability of the system, allowing for a payback period of less than 10 years. The first suggestion involves reducing the O&M cost of the system by 19% at 43.9 €/MWh, and the second suggestion entails increasing the overall efficiency of the system by 20%. This system can save 787.7 kg of CO_2-eq/ton$_{\text{waste-wood}}$ and generate a total of about 0.8 million MWh of electricity each year. The findings provide scientific evidence for the design and deployment of the hybrid technology to enhance energy security, while reducing carbon emissions. Overall, this study highlights the potential benefits of hybrid solar-bioenergy systems and encourages the adoption of sustainable energy practices for a greener future.

1. Introduction

The depletion of fossil fuels and increasing greenhouse gas (GHG) emissions leading to climate change, are two of the major challenges that have promoted the search for renewable, low-carbon fuels and energy products [1]. Biomass and solar energy are two of the promising sources of renewable energy. Biomass has been used to generate electricity, heat, fuels, and chemicals through various methods; gasification is one of those methods that continues to receive constant attention for its high carbon conversion efficiency and excellent scalability. Meanwhile, solar energy is a clean energy source that has been used for heat production via concentrated solar towers (CSTs). A CST typically consists of thousands of heliostats reflecting solar radiation and focusing it onto a receiver at the top of the tower. The resulting solar thermal energy supply is dependent upon the local direct normal irradiation (DNI) value and the area of the heliostat field [2]. A CST is regarded as a highly efficient solar thermal collection technology which can provide temperatures of 800 to 1,500 °C; the resulting thermal energy is then available for other processes such as bioenergy production [3].

Recent studies have focused on combining solar thermal technologies with bioenergy technologies to achieve greater process efficiencies. Concentrated solar thermal gasification of biomass (CSTGB) is one example of these kinds of integrated technologies. Pramanik et al. [4] argued that a high-performance CSTGB system fully driven by solar energy has the capability to effectively reduce CO_2 emissions to below 100 kg/MWh for electricity generation. Due to the intermittency of solar energy, CO_2 emissions from the system increased to the levels of conventional gasifier during nighttime. To address this, the addition of a thermal storage system (*i.e.,* TES) is necessary. Puig-Arnavat et al. [5] emphasized that CSTGB systems are a compelling and noteworthy alternative to conventional gasification processes and have the ability to produce high-quality gas with impressive yields. Fang et al. [1] has been shown that CSTGB could increase the utilization rate of biomass feedstock by 25–50%. The quality of the product gas, and reduction of pollutant emissions (*e.g.,* NO_x, PM_{10}, and VOCs) appears beneficial, compared to other conventional bioenergy processes [6]. High system

* Corresponding author.
E-mail address: siming.you@glasgow.ac.uk (S. You).

https://doi.org/10.1016/j.energy.2023.128709
Received 12 April 2023; Received in revised form 5 August 2023; Accepted 8 August 2023
Available online 9 August 2023
0360-5442/

efficiency is critical for the economics and widespread implementation of renewable energy generation. The heat required for conventional gasification is supplied by the partial combustion of the feedstock, while for CSTGB, the solar energy is utilized for the gasification process, which contributes to reduce the GWP and production costs, and increase electricity production and project revenue [7].

CSTGB systems have been proven to be efficient and cost-effective, while meeting current environmental emission regulations [8]. However, the operational characteristics of a CSTGB system limits its application to base loads, and the system needs to combust part of the feedstock to heat the gasifier at night or hours of low solar radiation [9]. A thermal energy storage (TES) system can be integrated with the CSTGB system to mitigate the issue of solar discontinuity and to provide continuous thermal energy for the gasification reaction at night, guaranteeing 24/7 operation of the system. It can also improve the overall efficiency of the CSTGB system and increase the electricity production, and reduce the CO_2 onsite emissions [10]. TES direct storage technologies can be classified as either sensible or latent heat. Sensible thermal energy storage (STES) has the potential to play an important role for low-cost thermal storage [11]. The core of STES technology is the use of heat storage and transfer materials (*e.g.,* sand and rock) and their properties (*e.g.,* heat capacity, molten point, and thermal transfer efficiency) that affect the efficiencies of thermal storage and release [12].

The main product of the CSTGB system is producer gas (*i.e.,* a mixture of H_2, CH_4, CO, and CO_2) [1]. The producer gas needs to be purified through a filtration unit before storage. The properties of H_2 (*i.e.,* flammable, explosive, and difficult to store) pose some safety risks and increase the capital and maintenance costs of H_2 storage [13]. To avoid these problems, the producer gas from a CSTGB system can be fed directly into a combined cycle gas turbine (CCGT) to convert the chemical energy of the synthesis gas to electricity. This method has been demonstrated in power systems as a reliable and highly efficient technology for electricity generation (67.9% thermal efficiency and 42.6% exergy efficiency not including carbon capture). Thus, the issue of producer gas storage can be alleviated [14].

The CSTGB concept was developed by Modell et al. [15] in 1978. Subsequently, research institutions in the USA, Japan, Germany, and China have conducted extensive research on various scientific and technical issues (*i.e.,* costs, performance, and onsite emissions) of CSTGB systems. The first CSTGB system, Plataforma Solar de Almeria (PSA), was successfully established in 2002 and generated 230 kWh of electricity [16]. A CSTGB system with a capacity of 30 kg/h was built at Enschede, Netherlands, in cooperation with the European Union and Japan, in 2004, and it achieved a producer gas yield over 2 $L/g_{wood\ sawdust}$ [17]. Another CSTGB system with a capacity of 1 ton/day of waste wood and a system efficiency of 70% was built at Hiroshima University, Japan [18]. In 2007, Kuste et al. [19] built a pilot-scale CSTGB system in Germany ('VERENA') with a design capacity of 100 kg/h of biomass and 77 vol% hydrogen concentration of producer gas. Yakaboylu et al. [20] introduced a fluidized bed reactor into the CSTGB system at the Delft University of Technology in the Netherlands in 2018, which reached a maximum feeding rate of 50 kg/h with the highest carbon conversion efficiency of 73.9%. A larger commercial CSTGB system with a designed capacity of 200 kg/h of biomass slurry was built to generate electricity by the General Atomics Company in the USA [21].

Although CSTGB systems have proven to be highly efficient, their environmental and economic benefits should be clarified before commercialization and large-scale implementation [22–25]. Life cycle assessment (LCA) is a structured, standardized method for quantifying the environmental impact of a technology, system, or service throughout its whole life cycle [26]. It can be used to evaluate the carbon footprint of electricity production from CSTGB systems and to compare the influences of feedstocks, solar radiation, the parameters of gasifier, and the capacity of CCGT for hot spotting. It can also be used to support decision-making for policy makers and support practitioners to optimize CSTGB development [27]. Chen et al. [21] conducted a LCA study of the CSTGB system with a capacity of 1ton/hr biomass, and it was shown that the system operation contributed approximately 58% to the total environmental impact. The greenhouse warming potential (GWP) of the operation phase was 4.4 $kgCO_2$-eq/kgH_2; the other 42% of the GWP came from the manufacturing phase (*i.e.,* raw material manufacturing, biomass collection, and material transport) and end of life phase (*i.e.,* dismantling the plant and demolishing the buildings). Banacloche et al. [28] studied the LCA of a CSTGB system with a TES system and carbon captured and storage (CCS) system in Tunisia, and the reported GWP was −77 $kgCO_2$-eq/MWh of electricity. Various approaches to the LCA studies currently exist [29,30], while the importance of method choice, emission types, and the contribution of individual life cycle stages has not been critically assessed in the context of CSTGB system power generation. A systematic overview of the consequences of technology choice and performance is needed to provide a transparent and balanced basis for future LCA modelling of CSTGB system power generation technologies.

The CSTGB system, integrated with TES and CCS subsystems, allows for stable 24/7 operation and lower onsite CO_2 emissions [1]. However, previous studies have shown a 30% higher capital cost of construction, and a higher operation & maintenance (O&M) cost (17.8 €/MWh) for the integrated system as compared to CSTGB systems without TES and CCS subsystems [31]. The CBA is one of the methods of economic analysis which is needed to evaluate, compare, and determine the selection of the project. It is used to determine the benefits of the project, compares the required investment and costs, and identifies the actions needed to maximize the return [32].

Cost benefit analysis (CBA) has been widely used to assess the economic viability of biomass, waste, and energy-related projects or schemes [33]. By systematically analyzing and comparing benefits and costs, it answers questions such as whether a proposed project or scheme is worthwhile. The CBA serves as an effective tool for making decisions about the use and allocation of society's resources [34]. However, existing CBA studies regarding CSTGB systems have demonstrated that the electricity generated by CSTGB was hardly affordable for end users [35,36], which is challenging for the long-term viability of these systems. There are no comprehensive studies to assess the environmental sustainability and economic analysis of CSTGB systems, which are crucial for the decision-making process of policy makers and investors.

This paper fills this knowledge gap by studying the environmental impacts and economic feasibility of CSTGB development in Spain. LCA and CBA were carried out based on the proposal of an all-weather and 24/7 operational CSTGB system consisting of 4 main subsystems, namely CST, TES, downdraft fixed bed gasifier, and CCGT with CCS. Waste wood is considered as feedstock, and is resourced from three cities (*i.e.,* Seville, Cordoba, and Malaga). This study presents a holistic understanding of the system's environmental performance and economic feasibility, contributing valuable insights to the field of CSTGB development and sustainable energy solutions.

2. Methodology and materials

A schematic illustration of the methodology including system design, LCA, and CBA is shown in Fig. 1. For the system design, thermodynamic analysis was carried out to decide the gasifier specification (includes reaction temperature, thermal energy demand, and equivalence ratio) and SolarPILOT software was used to determine the heliostat specification (*i.e.,* area and layout) and the CST receiver specification (*i.e.,* the surface area of receiver and tower height), followed by the use of our recent model [37] to decide the optimal process conditions to achieve maximum synthesis gas production. The information of process conditions and system configurations were then used in the LCA and CBA to evaluate the GWP and economic viability of CSTGB development.

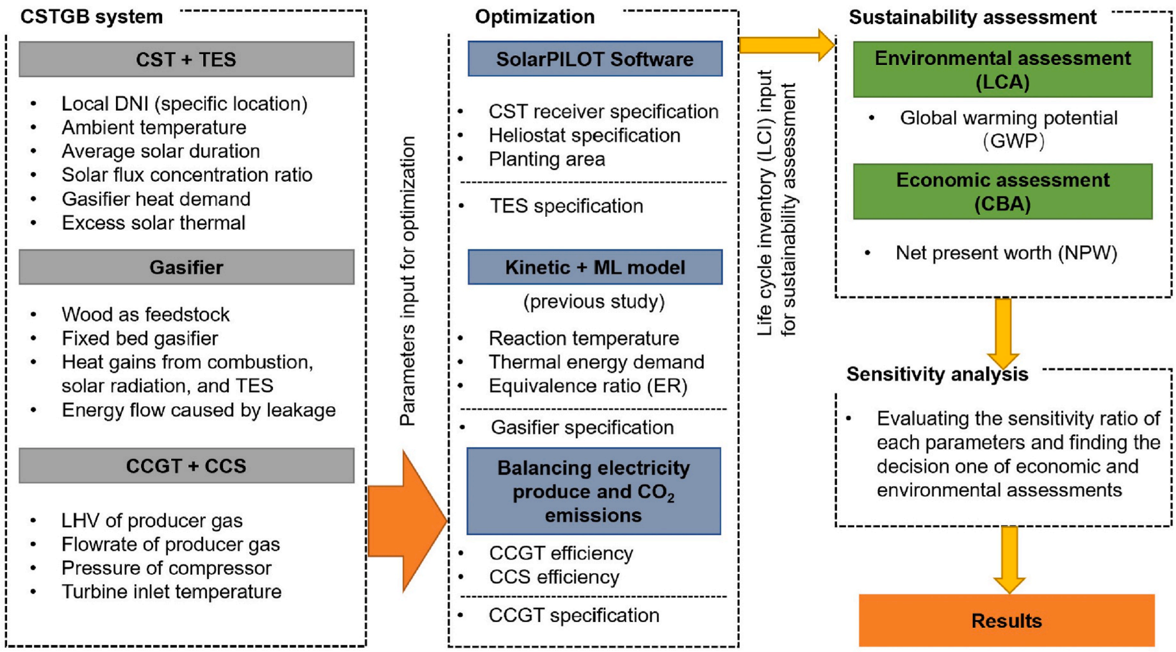

Fig. 1. The schematic illustration of the methodology. CSTGB: concentrated solar thermal gasification of biomass; CST: concentrated solar tower; TES: thermal energy storage; CCGT: combined cycle gas turbine; CCS: carbon captured system; ML: machine learning; LCA: life cycle assessment; CBA: cost benefit analysis; DNI: direct normal irradiation; LHV: low heating value.

2.1. *Thermodynamic analysis of the CSTGB system*

2.1.1. *Description of the CSTGB system*

The proposed CSTGB system is powered by a synergistic thermal energy supply method that combines thermal energy from the partial feedstock combustion and the solar thermal energy from a CST subsystem and stored thermal energy from a TES subsystem. Fig. 2 presents a schematic illustration of the proposed CSTGB system. The combination minimizes the impact of extreme weather conditions (*e.g.,* insufficient solar radiation in winter and absence of solar radiation at night) on the system. The heliostat field area, the size of the CST receiver, and the scale of the TES subsystem are determined by the local DNI and the thermal energy demand of the gasifier. The excess solar thermal energy is stored into the TES subsystem and supplied to the gasifier as a backup. The performance of the TES subsystem is dependent on its thermal storage and insulation materials [38]. Stone wool has been considered as the insulation material of the TES subsystem to minimize thermal energy loss. Quartz sand is used as both a heat transfer medium and heat storage material with a specific heat capacity of 0.83 kJ/(kg K); it has a high melting point of 1,577 °C that avoids phase change and reduces the system complexity [39]. A screw transfer machine (STM) is used to transport the sand carrying thermal energy to the TES subsystem and to the heat exchanger inside of the gasifier. Here, we consider the gasifier has 5% gas leakage [40] and it is an indirect reactor of gasification in which the quartz sand and biomass particles are not mixed to avoid the separation process of sand and biomass/biochar particles. The high-quality producer gas with a higher low heating value (LHV) is the main product of the CSTGB system, and it is fed into the CCGT subsystem to generate electricity (the overall efficiency of the system $\eta_{system\_overall}$ is used to assess the energy conversion performance of the system, *i.e.,* from biomass feedstock and solar energy to electricity) after tar and fine particle removal by a gas cleaning unit. In addition, CO_2 as the by-product of the CSTGB system is captured by a CCS subsystem, which minimizes the onsite CO_2 emission.

The autothermal reaction in the gasifier was taken into consideration as a backup to prevent a circumstance where the solar thermal energy and stored thermal energy are insufficient to properly drive the gasification process. In a previous study [37], a single particle shrinkage core-based kinetic gasification model was proposed and combined with the Monte Carlo simulation and a Random Forest algorithm to predict optimal gasification process conditions with the aim of the maximum producer gas (*i.e.,* syngas) production. The model has also been applied to study the influences of various parameters (*e.g.,* water content, particle size, porosity, thermal conductivity, emissivity, shape, and reaction temperature) on producer gas production. It was found that reaction temperature had the most significant impact on gas production and quality. The model was applied in this work to determine the maximum producer gas yield and associated process conditions [37]. Wood – chemical compositions are presented in Section 2.2.2 – and considered as feedstock, associated with an optimum reaction temperature of 800°C and a 10% heat loss rate for the air fixed-bed gasifier. The effects of air equivalence ratio (ER) on the flow rate, LHV, cold gas efficiency (CGE),

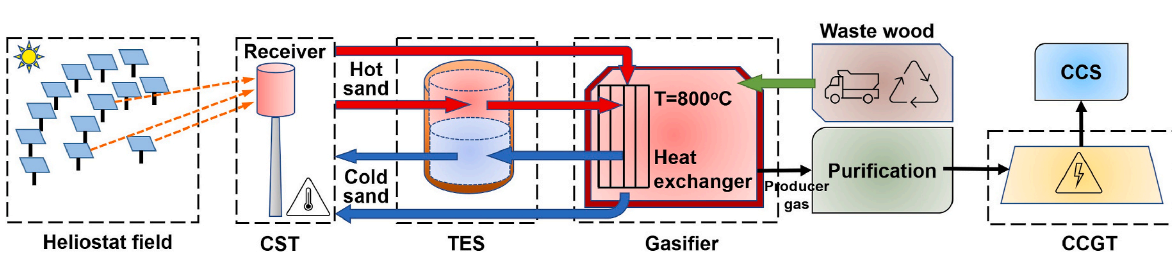

Fig. 2. The schematic diagram of the proposed CSTGB system.

and composition of the producer gas are shown in Fig. 3, in which the optimum reaction temperature was maintained by controlling the air supply. It was shown that the CO_2 concentration in the producer gas increased as the ER value increased up to 0.3, whereas the CGE and LHV decreased.

2.1.2. Location

The proposed CSTGB system was assumed to be built in Seville, Spain (Lat: 37.5°, Lon: −5.3°). Seville was selected due to its significant wood waste accumulation, accounting for 73% of the country's annual wood waste generation [41]. This amounts to around 8 million tons, representing 1.3% of the global annual wood waste volume [42]. Spain is one of the European countries which are most suitable for the development and implementation of solar power technologies with solar radiation levels of 1,600–1,950 kW/m^2 [43]. The considered typical meteorological year (TMY) data of this location includes the hourly DNI, global horizontal irradiance (GHI), ambient temperature, and relative humidity. The average DNI value is 641.4 W/m^2 and the annual sunshine hours are 3,966 h. The Photovoltaic Geographical Information System (PVGIS) from European Commission [44] was used to obtain the data of wind direction, wind speed, and precipitation in this location (reference data from 2005 to 2020). It was found that this location was dominated by northeasterly winds of 4–5 km/h from March to August and southeasterly winds of 3–4 km/h from February to September. The precipitation was sparse with an average of 53.4 mm/month. The lower wind speeds and rare precipitation allowed the designed CSTGB system to be constructed without extensive insulation materials. Steam as a gasifying agent is less practicable than other agents (*i.e.,* air, O_2, and CO_2) due to the scarcity of water resource. The use of O_2 and CO_2 would require capture and compression with specialized equipment, which would increase the cost and GWP of transportation [45]. As a result, air was deemed the most suitable gasifying agent for the proposed CSTGB system.

Wood is one of the most popular construction materials in Spain, resulting in a high proportion of waste wood being produced each year from construction and civil works [46]. Waste wood was considered as the biomass feedstock for the CSTGB system. Waste wood production increased from 1 to 1.6 million tons per year from 2001 to 2010 and continues to increase. Millions of tons of CO_2 are annually emitted into the environment as a results of it being burnt and landfilled [46]. The European Environment Agency (EEA) reported that Spanish government paid 50 €/ton (approximately €8 million per year) as gate fees to collect, store, and landfill waste wood [47]. The average distance from the location of the proposed CSTGB system to the waste wood collection point in the surrounding cities was found to be 100 km (to Seville is 70.1 km, to Cordoba is 82.5 km, and to Malaga is 155 km). The captured CO_2 and ash will be transported back to the wood waste recycling center [48] in the surrounding cities, ensuring a direct integration into the subsequent processing and utilization stages. This allows an efficient and coordinated flow of materials, enabling optimal utilization of waste wood resources and minimizing environmental impacts.

2.2. Life cycle assessment

LCA is a standardized approach for assessing the environmental impacts of a given process, technology, system, or service throughout its whole life cycle. LCA is defined by the ISO 14000 series of international standards, which consists of principles and framework (ISO 14040), goal and scope definition and inventory analysis (ISO 14041), life cycle impact assessment (ISO 14042), life cycle interpretation (ISO 14043), and requirements and guidelines (ISO 14044) [49].

2.2.1. Goal and definition

The goal of the LCA is to evaluate the GWP of the CSTGB system to be deployed in Sevilla, Spain and apply the information for planning waste wood treatment and renewable generation. Fig. 4 illustrates the boundary of the LCA, which encompasses all pertinent processes within the system. The LCA system boundary includes sub-process such as CO_2 emission from diesel refinery, onsite CO_2 emission, CO_2 captured by CCS subsystem, transportation of waste wood, and electricity generated from the proposed CSTGB system. The functional unit defined in this study is the treatment of 1 ton$_{\text{waste-wood}}$. The entire LCA is conducted in accordance with ISO 14040 with a commercial LCA software GaBi and Ecoinvent 3.0 database [50]. Two cases were compared: case 1 uses with both the CST and TES subsystems and case 2 uses without the CST and TES subsystems, which will create knowledge about the relative effectiveness of CST and TES on the development. In the proposed CSTGB system, the captured CO_2 is not used on-site, it undergoes compression and transportation by truck to the recycling center for further processes (*i.e.,* injection into deep geological formations). The treatment (*i.e.,* recovery and utilization) of the ash, generation and collection processes of wood waste are excluded from the system boundary.

2.2.2. Life cycle inventory analysis

Waste wood from construction and civil works (as mentioned in Section 2.1.2) was dried pretreated and transported by truck to the location of the proposed CSTGB system. The chemical composition of the waste wood (50.3 wt% carbon, 7.8 wt% hydrogen, 41.8 wt% oxygen, 0.1 wt% nitrogen, the high and low heating value are 20.6 and 18.7 MJ/kg) was assumed to be the same as the wood pellet reported by an existing study [51]. The processing capacity of the proposed CSTGB system was assumed to be 1,700 tons per day according to the system

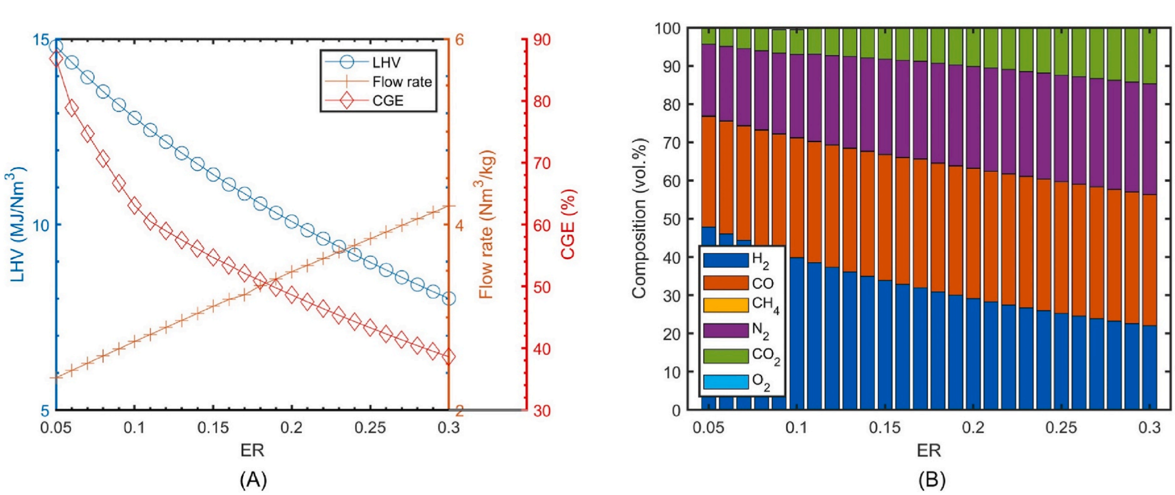

Fig. 3. (A) Effects of ER on producer gas flow rate, producer gas LHV, and system CGE; (B) Effects of ER on producer gas composition.

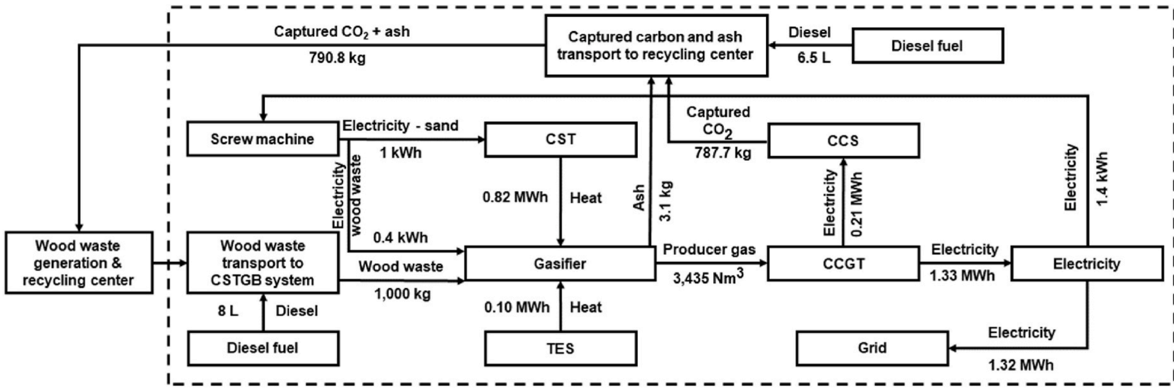

Fig. 4. LCA boundary of the CSTGB system.

scale.

The specifications of the CST subsystem were determined based on a gasification reaction temperature of 800 °C and a local average DNI value of 641.4 W/m^2 (as mentioned in Section 2.1.1 & 2.1.2). The default environmental parameters (*i.e.,* incidence angle, ambient humidity, and cloud thickness) was optimized using the software SolarPILOT [52]. The optimized values were 151,488 m^2 for heliostat field area, 30 m^2 for receiver area, 80 m for receiver tower height, 71.7% for solar thermal efficiency of the CST subsystem. The heliostat field layout and the position of each heliostat are depicted in Fig. 5. The area of a single heliostat in the CST subsystem was decided based on a life cycle cost analysis by Bhargav et al. [53]. The area of 120 m^2 was found to be more suitable for the CSTGB system in terms of economic applicability than that of 64, 96, and 148 m^2.

The 300-MW_{th} capacity of the TES subsystem was determined by the required peak thermal energy storage of 296.1 MW_{th} calculated based on the day (22 June) featured by the longest solar time and the highest DNI value as shown in the TMY dataset.

The heat transfer efficiency from quartz sand to the feedstock within the gasifier was supposed to be 100% since the reactions inside the gasifier were considered in thermal equilibrium, indicating maximum energy conversion. An input temperature of 1,010 °C and an output temperature of 750 °C were calculated for the quartz sand for a gasification reaction temperature of 800 °C. The CCGT subsystem was employed to convert producer gas to electricity. The efficiency of the producer gas-fueled CCGT with an CCS subsystem was within a range of 10.8–19% and the CCS subsystem consumed 30% of gross power output [54].

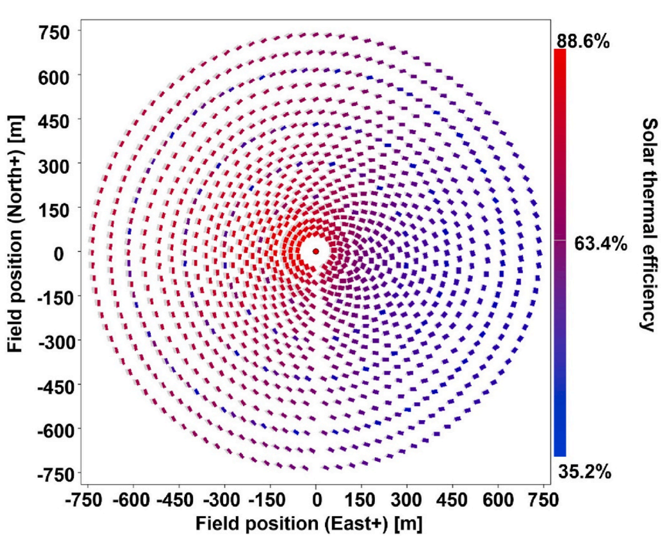

Fig. 5. The optimal heliostat field layout of the CST subsystem.

Two distinct STMs were used in the CSTGB system. The gasifier received the waste wood through Machine I (designed for a transportation distance of 10 m). Quartz sand was moved between the CST, TES, and gasifier subsystems using Machine II (designed for a transportation distance of 284.7 m). Heat losses of all subsystems and screw pipeline were assumed to be 10% [55]. Table 1 summarizes the specific design parameters of the proposed CSTGB system.

The material consumption of each subsystem of the CSTGB system are listed in Table 2. Chromium steel (melting point of 1,860 °C) was used as the construction material because of its capability to withstand the CST receiver and CCGT subsystems' operation temperature of 1,111–1,288 °C. The TES subsystem, gasifier, and screw pipe were built using reinforcing steel that has a melting point of 1370 °C. Material losses during construction of the CSTGB system, power consumption during assembly, and emissions and energy consumption associated with demolition of the system were not included, as studies have shown that their contribution towards emissions and energy were negligible compared to operation [7].

2.2.3. Life cycle impact assessment

To comprehensively evaluate the environmental impact of the CSTGB system, a life cycle impact assessment (LCIA) was conducted using the GaBi software (as mentioned in Section 2.2.1). The LCIA process entails categorizing the LCI data into specific impact categories and corresponding indicators that elucidate the causal relationship between the system's activities and its environmental impacts. The ReCiPe Midpoint V1.08 methodology was adopted to calculate the GWP of the CSTGB system which quantifies the total greenhouse gas emission associated with the system over a 100-year time (*i.e.,* GWP 100) horizon.

2.2.4. Data interpretation

Based on the LCIAs adopted in Section 2.2.3, the environmental impact (*i.e.,* GWP) for the proposed CSTGB system was discussed, which included identification of carbon emission [63]. A sensitivity analysis was performed to assess the influence of parameter (*i.e.,* CCS subsystem's efficiency, onsite emission, gasifier leakage, transportation, and diesel at refinery) variations (range of ± 10%). The sensitive ratio (SR), defined as Eq. (1), was used to quantify the influences. According to the study by Zahra et al. [64], when SR > 0.2, this indicates a high degree of influence of the factor on the results; when SR < 0.2, it is considered that the factor limited influence on the results (*i.e.,* GWP).

$$SR = \left| \frac{\frac{\varphi_i^b - \varphi_i^m}{\varphi_i^b}}{\frac{\Phi_i^b - \Phi_i^m}{\Phi_i^b}} \right| \tag{1}$$

where φ indicates the GWP value, and Φ indicates the value of each

Table 1
Design parameters of the proposed CSTGB system.

Item	Value (unit)	Adapted based on data from existing studies or calculated
Location	Lat: 37.5 °, Lon: −5.3 °	
Altitude	169.0 m	[44]
DNI	641.4 W/m^2	[44]
Ambient temperature	19.1 °C	[44]
Designed solar receiver temperature	1,111.0 °C	[44]
Average solar duration	7.9 h	[44]
Solar flux concentration ratio (C)	3621.6	calculated
CST receiver specification		
Receiver type	External cylindrical	[56]
Receiver height	4.8 m	[56]
Receiver diameter	4.7 m	[56]
Receiver area	30 m^2	[56]
Tower height	80 m	calculated
Optical efficiency (at receiver)	71.7%	calculated
Heliostat specification		
Single heliostat width	12 m	[53]
Single heliostat height	10 m	[53]
Single heliostat area	120 m^2	[53]
Heliostat field	151,488 m^2	calculated
Number of single heliostats	1,263	calculated
TES specification		
Number of tanks	1 integrated tank	[57,58]
Tank type	External cylindrical	[57,58]
Tank height	20 m	calculated
Tank diameter (with 0.1 m insulation layer)	10.5 m	calculated
Numbers of hours of TES	16.1 h	calculated
Capacity of the TES	300 MW_{th}	calculated
TES heat loss	10%	[55]
Temperature of TES	448.1 °C	calculated
HSM of TES	Quartz sand	[39]
Total sand weight	1,245.5 t	calculated
Total sand volume	1,660.3 m^3	calculated
Gasifier specification		
Gasifier type	Fixed bed	[25,57]
Gasifier agent	Air (O_2:21%, N_2:79%)	
Gasifier heat lose	10%	[55]
Equivalence ratio (ER)	0.05–0.3	calculated
Inlet temperature of quartz sand entrancing the gasifier	1,010°C	calculated
Gasification temperature	800 °C	calculated
Output temperature of quartz sand exiting the gasifier	750 °C	calculated
Required thermal energy to increase feedstock from the ambient temperature to 800 °C	1.1 $MJ/kg_{feedstock}$	[51]
Required thermal energy to increase air from the ambient temperature to 800 °C	1.0×10^{-6} MJ/kg_{air}	[51]
Total thermal energy needed by the gasifier	4.7 $MJ/kg_{feedstock}$	[51]
CCGT specification		
Electricity efficiency with CO_2 capture	10.8–19% (depend on LHV of producer gas)	calculated
CO_2 capture efficiency	90%	[57,59,60]
Pressure ratio of GT compressor	19	[57,59,60]
Turbine inlet temperature	1,288 °C	[57,59,60]
Turbine exhaust temperature	544.2 °C	[57,59,60]
Parameters of the high-pressure steam	521.2 °C/55 bar	[57,59,60]
Parameters of the low-pressure steam	260.2 °C/6.9 bar	[57,59,60]
Screw machine specification		
Machine-1 for feedstock input		
Screw diameter	1 m	[61]
Screw pitch	0.6 m	[61]
Rotational speed	50 rpm	[61]
Conveying capacity	608 m^3/h	calculated
Power	96 kW	calculated
Machine-2 for sand transfer		
Screw diameter	0.6 m	[61]
Screw pitch	0.5 m	[61]
Rotational speed	50 rpm	[61]
Conveying capacity	160 m^3/h	calculated
Power	159.7 kW	calculated
Screw pipe specification		
Screw pipe heat loss	10%	[55]
Pipe-1 for feedstock input		
Screw diameter	1 m	[61]
Length	30 m	calculated
Pipe-2 for sand transfer		
Screw diameter (with 0.025-m thickness insulation)	0.7 m	[61]
Length	284.7 m	calculated

factor, b indicates baseline value, and m indicates modified value.

2.3. Cost benefit analysis

The NPW approach was used to assess the economic viability of the proposed CSTGB system. All cash flows of the proposed CSTGB system are examined over 30 years and resolved to their equivalent present worth (PW) cash flow. Revenues were considered to be positive cash flows while costs were negative [65]. The NPW of the CSTGB system was calculated by Eq. (2)

$$\mathrm{NPW} = \mathrm{CAPEX} + \mathrm{PW(O\&M)} + \mathrm{PW(T)} - \mathrm{PW(ES)} - \mathrm{PW(CT)} \tag{2}$$

where CAPEX is the capital cost that included the initial investment cost of constructing of the CSTGB system, O&M is the operation and maintenance cost, T is the cost of transporting the waste wood from the cities to the location of the CSTGB system, ES is the incomes from selling the renewable electricity, and CT is the incomes from carbon tax. The PW is the present value, which is calculated by Eq. (3) with annual value (AW).

$$\mathrm{PW} = \mathrm{AW}\frac{(1+i)^N - 1}{i(1+i)^N} \tag{3}$$

where i denotes the interest rate (an interest rate of 6% was used based on literature [65]), and N denotes the assumed operation years ($N = 30$ years in this study). The exchange rate of euro to US dollar was 1.13 and GBP to US dollar was 0.85 based on year 2019.

2.3.1. CAPEX and O&M cost

There was no existing CSTBG related plant that could be referred to about e.g., construction material costs and O&M costs. A process costing approach was used to calculate the CAPEX for each subsystem (*i.e.,* CST, gasifier, and CCGT) of the proposed CSTGB system which was summed to calculate the total CAPEX. Due to the inconsistency in the year of the referenced system, we used the Chemical Engineering Plant Cost Index (CEPCI) values to update the CAPEX of each subsystem to the year 2019 (calculated by Eq. (4)).

$$\mathrm{Cost}_m = \mathrm{Cost}_n\left(\frac{\mathrm{CEPCI}_m}{\mathrm{CEPCI}_n}\right) \tag{4}$$

where m and n represent the reference and base year, respectively.

The CAPEX of the heliostat field, receiver tower, and TES were considered. The CEPCI index of the reference year (2019) as 607.5 [66] was used to calculated the CAPEX of a single heliostat as €103 based on the study by Bhargav et al. [53] which considered €112.4 for the year 2015 (the CEPCI index is 556.8 [66]) and included mirrors, support structure, drivers, mirror modules, driver control system, field

Table 2
LCI for the construction stage of the CSTGB system. The data are normalised based on the functional unit (*i.e.,* 1 $ton_{waste\text{-}wood}$).

Construction materials					
Material type	Component	Value	Unit	Normalised value	Unit
Installation of CST [58]					
Heliostat					
Flat glass coated, RER	Mirror	1,514,887.2	kg	8.1×10^{-2}	$kg/ton_{waste\text{-}wood}$
Reinforcing steel, RER	Steel structure	5,335,432.8	kg	0.3	$kg/ton_{waste\text{-}wood}$
Concrete, sole plate and foundation, CH	Concrete foundation	3,938.7	m^3	2.1×10^{-4}	$m^3/ton_{waste\text{-}wood}$
Receiver					
Chromium steel 18/8, RER	Receiver surface	5,990	kg	3.2×10^{-4}	$kg/ton_{waste\text{-}wood}$
CST tower (80 m)					
Concrete, sole plate and foundation, CH	Tower concrete	6,200	m^3	3.3×10^{-6}	$m^3/ton_{waste\text{-}wood}$
Excavation, hydraulic digger, RER	Tower excavation	4,200	m^3	2.3×10^{-4}	$m^3/ton_{waste\text{-}wood}$
Reinforcing steel, RER	Tower steel	1,200	kg	6.5×10^{-5}	$kg/ton_{waste\text{-}wood}$
Installation of TES [58]					
Steel, chromium steel 18/8, hot rolled	TES structure	582,232	kg	3.1×10^{-2}	$kg/ton_{waste\text{-}wood}$
Stone wool	TES insulation material	261,116	kg	1.4×10^{-2}	$kg/ton_{waste\text{-}wood}$
Installation of gasifier [62]					
Reinforcing steel, RER	Steel structure	10,000,000	kg	0.5	$kg/ton_{waste\text{-}wood}$
Steel, low-alloyed, RER	Steel structure	6,040,000	kg	0.3	$kg/ton_{waste\text{-}wood}$
Chromium steel 18/8, RER	Steel structure	16,400,000	kg	1.3×10^{-2}	$kg/ton_{waste\text{-}wood}$
Steel, electric, n-and low-alloyed, RER	Steel structure	242,000	kg	0.9	$kg/ton_{waste\text{-}wood}$
Concrete, normal, CH	Concrete foundation	94,900	m^3	5.1×10^{-3}	$m^3/ton_{waste\text{-}wood}$
Aluminum, primary, RER	Aluminum structure	889,000	kg	0.5	$kg/ton_{waste\text{-}wood}$
Aluminum, secondary, from new scrap, RER	Aluminum structure	105,000	kg	5.6×10^{-3}	$kg/ton_{waste\text{-}wood}$
Aluminum, secondary, from old scrap, RER	Aluminum structure	52,400	kg	2.8×10^{-3}	$kg/ton_{waste\text{-}wood}$
Brass, CH	Plant material	108,000	kg	5.8×10^{-3}	$kg/ton_{waste\text{-}wood}$
Stone wool, CH	Insulation material	1,730,000	kg	9.3×10^{-2}	$kg/ton_{waste\text{-}wood}$
Glass fiber, RER	Plant material	242,000	kg	1.3×10^{-2}	$kg/ton_{waste\text{-}wood}$
Polyvinyl, HDPE, granulate, RER	Plant material	69,300	kg	3.7×10^{-3}	$kg/ton_{waste\text{-}wood}$
Polypropylene, granulate, RER	Plant material	34,700	kg	1.9×10^{-3}	$kg/ton_{waste\text{-}wood}$
Styrene-acrylonitrile copolymer, RER	Plant material	11,600	kg	6.2×10^{-4}	$kg/ton_{waste\text{-}wood}$
Flat glass, uncoated, RER	Plant material	11,700	kg	6.3×10^{-4}	$kg/ton_{waste\text{-}wood}$
Cast iron, RER	Plant material	435,000	kg	2.3×10^{-2}	$kg/ton_{waste\text{-}wood}$
Epoxy resin, liquid, RER	Plant material	91,700	kg	4.9×10^{-3}	$kg/ton_{waste\text{-}wood}$
Lubricating oil, RER	Plant material	384,000	kg	2.1×10^{-2}	$kg/ton_{waste\text{-}wood}$
Synthetic rubber, RER	Producer gas pipe	52,600	kg	2.1×10^{-3}	$kg/ton_{waste\text{-}wood}$
Installation of CCGT [57]					
Reinforcing steel, RER	Steel structure	12,367,316.8	kg	6.8	$kg/ton_{waste\text{-}wood}$
Chromium steel 18/8, RER	Steel structure	162,612.5	kg	8.7×10^{-3}	$kg/ton_{waste\text{-}wood}$
Aluminum, RER	Aluminum structure	81,306.2	kg	4.4×10^{-3}	$kg/ton_{waste\text{-}wood}$
Concrete, sole plate and foundation, CH	Concrete foundation building	38,958,841.4	kg	2.9	$kg/ton_{waste\text{-}wood}$
Installation of pipes (314.7 m) [57]					
Reinforcing steel, RER	Steel pipe	189,185	kg	1.0×10^{-2}	$kg/ton_{waste\text{-}wood}$
Stone wool, RER	Insulation material	172.9	kg	9.3×10^{-6}	$kg/ton_{waste\text{-}wood}$

electronics, and wirings.

The CAPEX of the 100MWth CST subsystem was calculated to be €228,693,794.8, which covered the receiver, tower, TES, indirect costs (*i.e.,* owner cost and contingency), and site preparation as €52,963,596.7, €26,854,082.3, €74,598,612.4, €111,897,919.2, €22,379,583.6 for the year 2019, respectively (data provided by the International Renewable Energy Agency (IRENA) in the year 2018 [67] and the CEPCI index is 603.1 [66]. The annual O&M cost of the CST subsystem was 17.8 €/MWh, which included replacing receivers and single heliostats, heliostat washing (*i.e.,* water consumption), and factory insurance costs [31].

The integrated concept of gasifier and CCGT technologies has been proposed by several researchers [68–70]. The CAPEX of the 150 MW scale of the integral gasifier and CCGT system was calculated to be €171, 992,945.6 based on the National Renewable Energy Laboratory (NREL) report at the year 2008 [69] and the CEPCI index is 575 [66]. The data included gas cleanup facility, engineering fees, project contingency, and carbon capture costs [69]. The O&M cost of gasifier with a CCGT subsystem was based on a study by Cormos et al. [71], which concluded that the O&M cost of the gasifier with a CCGT subsystem was 36.37 €/MW in the year 2019. Thus, the total O&M costs of the proposed CSTGB system was calculated as 54.17 €/MWh.

2.3.2. Transportation cost

Transportation costs cover the purchasing of trucks, diesel cost, and the wages of the staff operating the truck. The CAPEX of each truck was €233,335 and the life cycle of 10 years, and the estimated annual O&M cost of 3,335 €/truck [65]. According to the fuel price report from Experian Catalist (http://www.catalist.com), the average diesel price was 1.26 €/L in Spain for the year 2019. The transportation cost can be converted to PW using Eq. (2). It was assumed that three staff are required to operate a truck with the wage as 15.0 €/h per person for the year 2019 (working 8 h per day) [72].

2.3.3. Electricity selling revenue

The electricity selling (ES) price was established based on market supply relationships, which include supplier and end-users (residential, commercial, and industry) [73]. Gracia et al. [74] assessed the Spanish market's willingness to pay for a portfolio of renewable electricity in 2010. Based on a consumer survey considering different genders, ages, education of respondent, average household monthly income, and household size, the local consumers (household, company, and industry) were willing to pay Feed-in Tariff (FiT) as 50 €/MWh and included tax for electricity from renewable resources [75].

2.3.4. Carbon tax revenue

Carbon tax (CT) is an effective policy and economic instrument to encourage the development of more environmentally friendly technologies for carbon abatement [76]. According to the literature [77], the CT price in Spain was established at 49.0 €/tCO_2 and used in the CBA of the designed CSTGB system.

2.3.5. Sensitivity analysis

Based on the CBAs adopted in Section 2.3.1 to 2.3.4, the economic viability (*i.e.,* NPW) for the proposed CSTGB system [63], a sensitivity analysis was conducted to evaluate the relative influences of different key factors (*i.e.,* CAPEX and O&M costs of the system, transportation costs, ES price, and CT) with variations (range of ± 10%). The sensitive ratio was also calculated using Eq. (3) with φ being the NPW value.

3. Results and discussion

3.1. Thermodynamic analysis

To better illustrate the daily operation of the proposed CSTGB system, the profiles of the thermodynamic performance for the system were obtained for March 19th, June 22nd, September 22nd, and December 21st, with the meteorological conditions, *i.e.,* local TMY data collected. The results are shown in Fig. 6.

It is shown in Fig. 6B that the most solar radiation was on June 22nd, and the gasifier could be completely powered by solar thermal energy from 07:00 to 17:00.248.6 MWh of solar thermal energy was stored in the TES subsystem (as shown in Fig. 6B), and the overall system efficiency ($\eta_{system\_overall}$) was 28.3%. During the period of insufficient solar radiation (18:00 to 6:00), the TES subsystem supplied 21.2 MWh of thermal energy to the gasifier, and an additional 71 MWh thermal energy was from the combustion of waste wood as required by the gasification process. The net electricity generation and the onsite CO_2 emission were 2,529.2 MWh and 63,175.7 kg on June 22nd (2,408.3 MWh and 67,688.6 kg on March 19th (Fig. 6A); 2,358.3 MWh and 70,700.0 kg on September 22nd (Fig. 6C). The least solar radiation was on December 21st (Fig. 6D): the total electricity generated was 2,241.2 MWh and the onsite CO_2 emission generated was 74,729.2 kg.

The monthly and cumulative electricity generation, CO_2 captured and stored, and onsite CO_2 emissions of case 1 and case 2 are shown in Fig. 7. It is shown that compared to case 2, the electricity output of case 1 increased by 203,485 MWh and the onsite CO_2 emission decreased by 155,552.3 tons. This means that using solar energy and TES subsystem significantly increased electricity production and reduced onsite CO_2 emission. In addition, the proposed CSTGB system (case 1) generate over 0.8 million MWh of electricity per year; it covered 0.31% of the total electricity consumption (about 260 TWh) in Spain during the year 2019 [78].

3.2. Environmental impacts

3.2.1. LCA results

The GWP results of case 1 and case 2 are shown in Fig. 8. In case 1 (Fig. 8A), the contributions of different components to the GWP of the CSTGB system are as follows: the CCS subsystem exhibited a significant carbon abatement potential, accounting for a carbon reduction of 116%

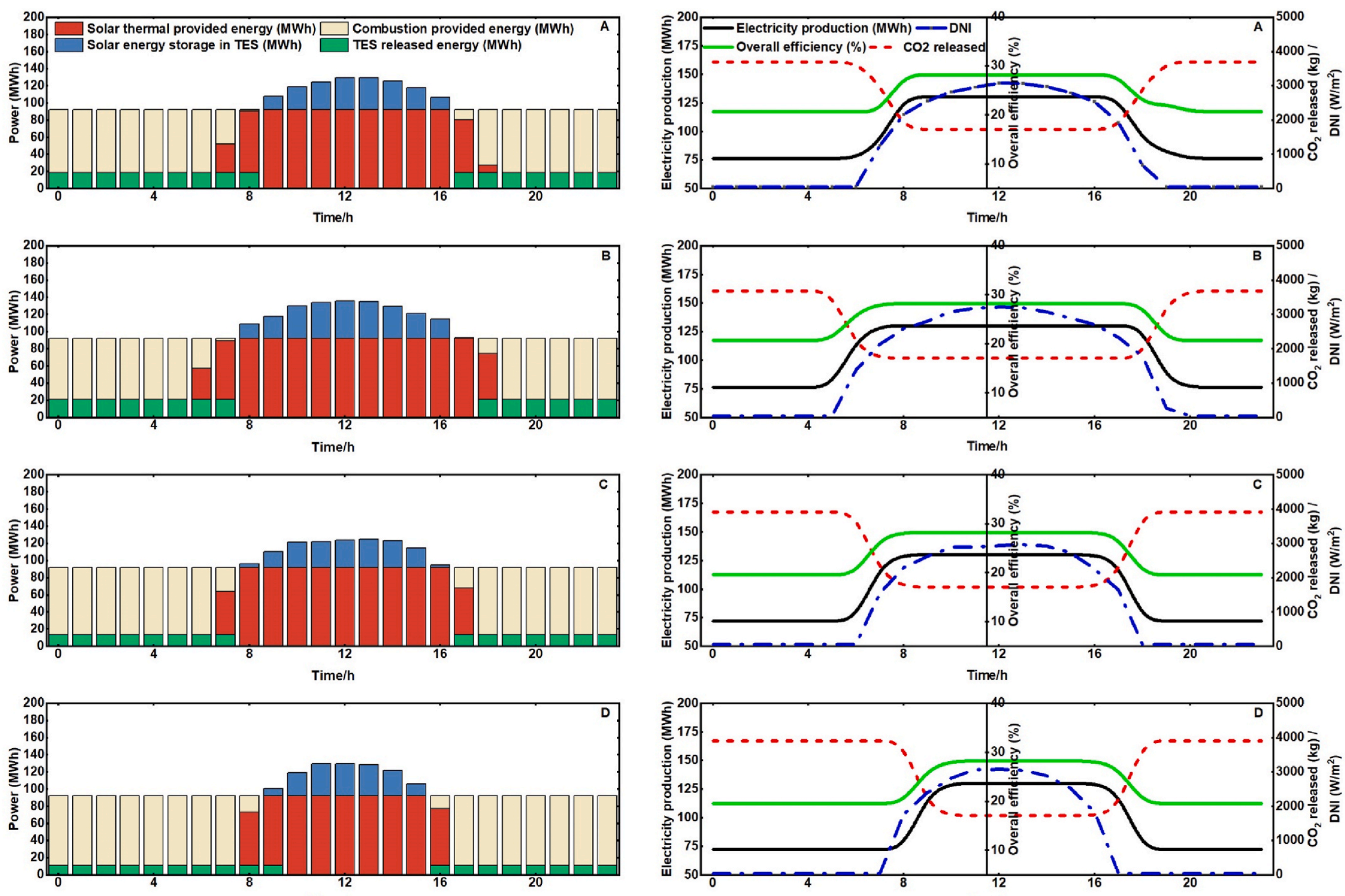

Fig. 6. Hourly net power and efficiency of the system in the representative days, (A). the day of March 19th, (B). June 22nd, (C). September 22nd, and (D). December 21st.

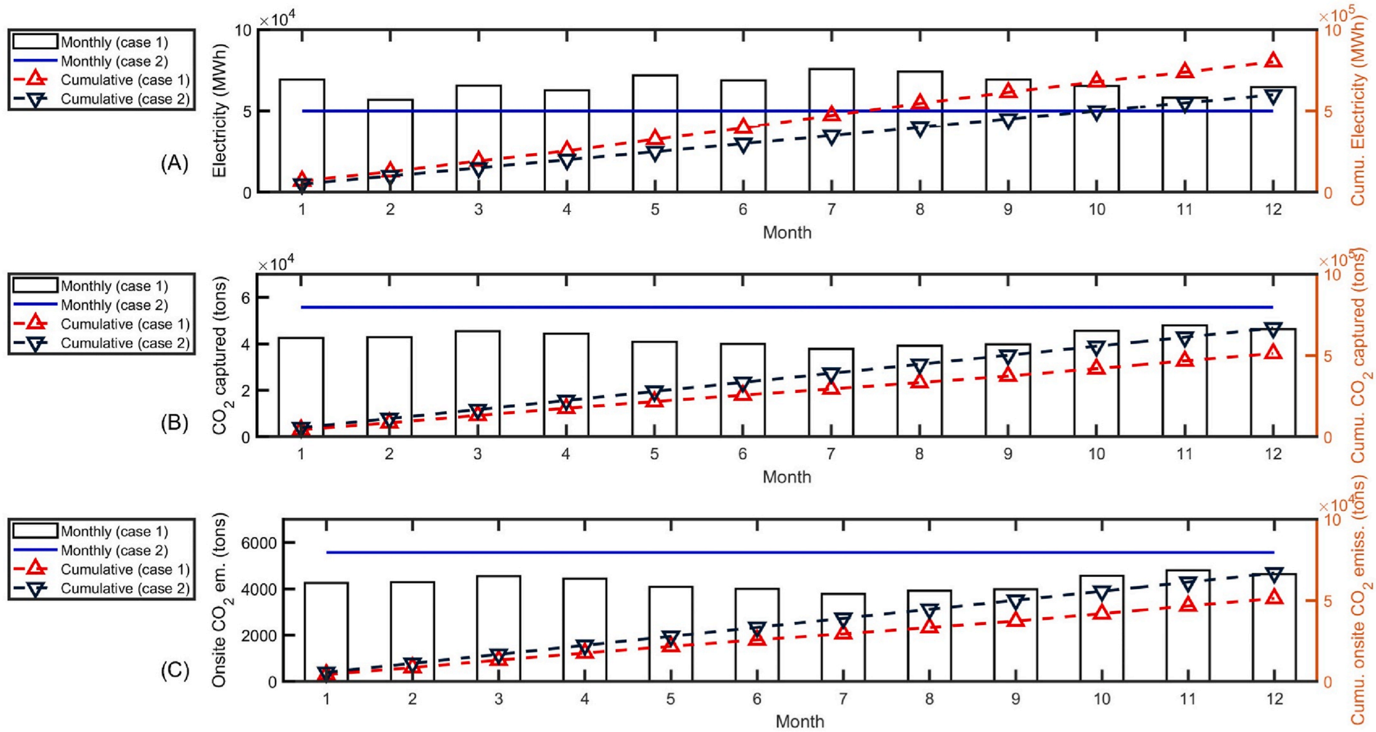

Fig. 7. Monthly and cumulative data: (A) electricity production, (B) CO_2 captured and stored, and (C) onsite CO_2 released to environment.

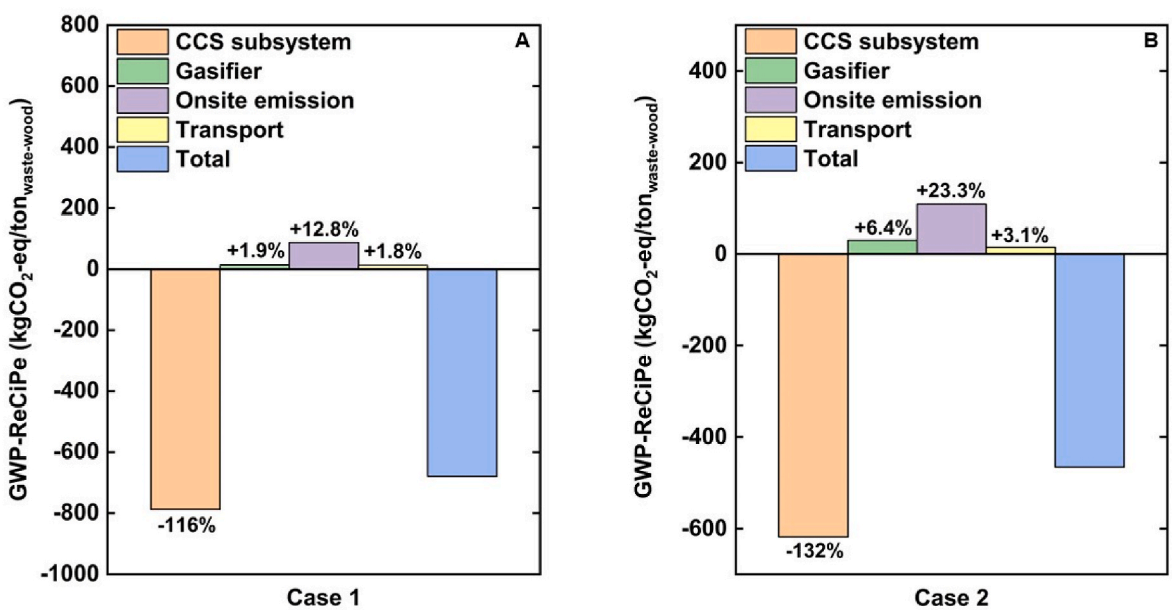

Fig. 8. Comparison of the GWP of case 1 (CSTGB system with CST and TES subsystems) and case 2 (without CST and TES subsystems), '+' represents positive impact on GWP value while '–' indicates carbon reduction.

with respect to the total GWP that is equivalent to −787.7 $kgCO_2$-eq/ton$_{waste-wood}$. Conversely, the gasification subsystem had a small positive carbon footprint, corresponding to a carbon emission of 1.9% that is equivalent to 13.2 $kgCO_2$-eq/ton$_{waste-wood}$. Onsite emissions including leakage and uncaptured CO_2 accounted for 12.8% of the total GWP that is equivalent to 87.5 $kgCO_2$-eq/ton$_{waste-wood}$. Similarly, transportation accounted for 1.8% of the total GWP that is equivalent to 12.3 $kgCO_2$-eq/ton$_{waste-wood}$. The total GWP is −678.6 $kgCO_2$-eq/ton$_{waste-wood}$. The GWP of case 1 was 212.7 $kgCO_2$-eq/ton$_{waste-wood}$ lower than that of case 2 (Fig. 8B) where the GWP of the CCS subsystem was accounted for a carbon reduction of 116% with respect to the total GWP that is equivalent to −618.7 $kgCO_2$-eq/ton$_{waste-wood}$. The gasification subsystem was responsible for a carbon emission of 6.4% that is equivalent to 29.8 $kgCO_2$-eq/ton$_{waste-wood}$. Onsite emissions constituted 23.3% (108.7 $kgCO_2$-eq/ton$_{waste-wood}$) of the total GWP, while transportation contributed 3.1% (14.2 $kgCO_2$-eq/ton$_{waste-wood}$) of the total GWP. The total GWP is −465.9 $kgCO_2$-eq/ton$_{waste-wood}$. The GWP of case 2 is similar to the study by Margaret et al. [79] which reported a GWP of −476.63 $kgCO_2$-eq/ton$_{feedstock}$ (that system assumed to have 90% carbon captured). This suggests that the proposed CSTGB system with CST and TES subsystems is more environmentally friendly from a carbon saving perspective.

3.2.2. Data interpretation

Fig. 9 illustrates the relevant impact factors on the GWP of the proposed CSTGB system, and shows that the SR of the CCS subsystem-related emission to be 0.37 and the SR of the onsite CO_2 emission to be 0.34, which were larger than 0.2 and the two most influential factors (as mentioned in Section 2.2.4). It is promising to reduce the carbon footprint of the proposed CSTGB system by improving the efficiency of the CCS subsystem. The GWP of the CSTGB development was less sensitive to the emissions related to transport (SR = 0.15), and gasifier (SR = 0.08).

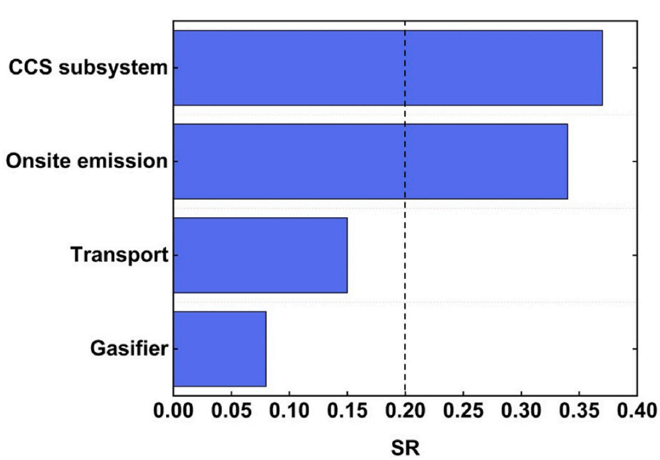

Fig. 9. Sensitivity analysis results (influences of major factors on the GWP of CSTGB).

3.3. Economic analysis

3.3.1. CBA results

The CBA results for the CSTGB system operating for 30 years are shown in Fig. 10. The total NPW was €–0.7 billion in year 30. The cumulative PW of the O&M cost of the CSTGB system was €6.4 billion in year 30. The PW of the transportation cost was €150 million, including €30 million for the wage of staff, €12 million for the CAPEX of the truck, and €780 thousand for the O&M cost, and €155 million for the diesel cost. The CAPEX of the CSTGB system was €461 million over the system's life cycle. The sources of revenue for the CSTGB system were CT and ES with the cumulative PW values being €0.3 billion and €6 billion, respectively. Here, the electricity selling price was assumed to be 50 €/MWh in Spain as mentioned in Section 2.3.3. The following two conditions need to be met for the proposed CSTGB system to be economically viable (based on a 10 year payback period): 1) the O&M cost of the system needs to be reduced 19% or 43.9 €/MWh or, 2) the overall efficiency need to be increased by 20%.

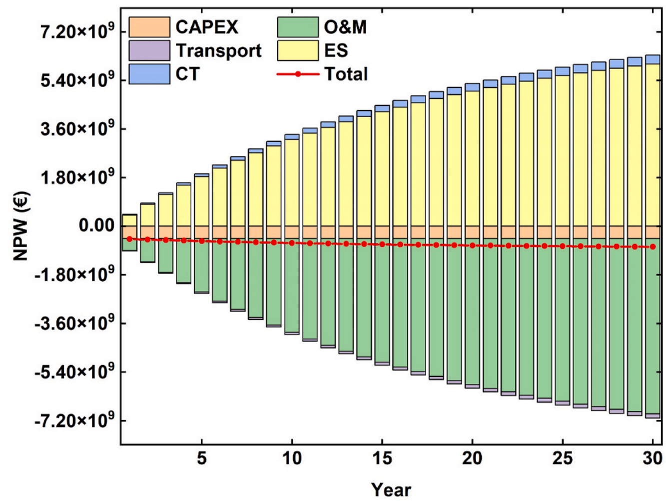

Fig. 10. PW and NPW results of the CSTGB system in the economic analysis.

3.3.2. Sensitivity analysis

The impacts of five factors (*i.e.,* CAPEX, O&M, transportation cost, ES, and CT) towards NPW were studied via sensitivity analysis, and the results are shown in Fig. 11. The O&M and ES emerged as the most influential factors, with the SR values of 0.37 and 0.34, respectively. Additionally, the CT (SR = 0.16), CAPEX (SR = 0.12), and transportation (SR = 0.08) had a relatively limited impact on the economic viability of the CSTGB system with all SR values below 0.2. It is expected that the O&M of CSTGB development would be further reduced [80]. Gracia et al. [74] found that the acceptable price of electricity from renewable resources was up to 440 €/MWh in Spain. Hence, there is great potential that the profitability of the CSTGB system would be significantly improved for a lowering O&M cost and a higher ES revenue.

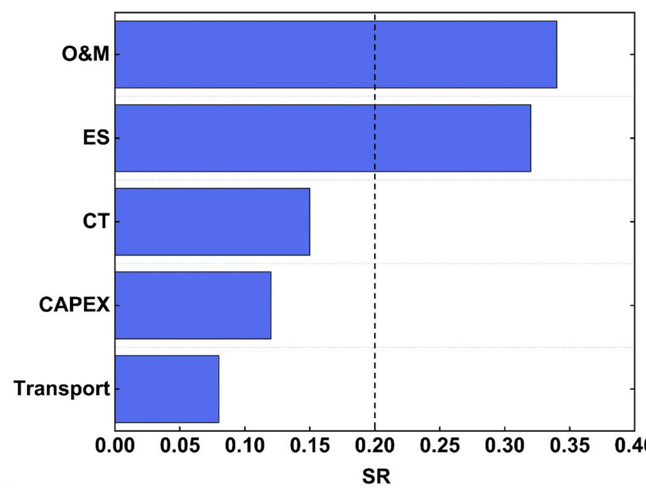

Fig. 11. Sensitivity analysis results (influences of major factors on the NPW of CSTGB).

4. Conclusions

The CSTGB system has a great potential to reduce the carbon footprint of electricity generation. The LCA results showed that the proposed CSTGB system could save over 0.5 million tons carbon emission (GWP = -787.7 $kgCO_2$-eq/$ton_{waste\text{-}wood}$) and generate over 0.8 million MWh of electricity per year, which could covers 0.31% of the total electricity consumption (about 260 TWh) in Spain in the year 2019. The results of the sensitivity analysis regarding LCA showed that the GWP of the proposed CSTGB system was primarily affected by the efficiency of the CCS subsystem. The CBA results showed that the total NPW in the 30th year was about €–0.7 billion, which is not profitable (the payback period was over 30 years). The results of the sensitivity analysis showed that the economic viability was mainly affected by the local ES price and the O&M cost. However, there was a great potential to make the system economically viable for a payback period shorter than 10 years when the O&M cost of the system could be reduced by 19% which equals 43.9 €/MWh or the overall efficiency of the system could be increased by 20%.

Credit author contributions

Yi Fang: Conceptualization, Data curation, Formal analysis, Investigation, Methodology, Validation, Writing – original draft. **Xian Li**: Conceptualization, Methodology, Validation, Writing – review & editing. **Simon Ascher**: Writing – review & editing. **Yize Li**: Writing – review & editing. **Leilei Dai**: Writing – review & editing. **Rogar Ruan**: Writing – review & editing. **Siming You**: Supervision, Conceptualization, Funding acquisition, Investigation, Project administration, Validation, Writing – review & editing.

Declaration of competing interest

The authors declare that they have no known competing financial interests or personal relationships that could have appeared to influence the work reported in this paper.

Data availability

A data availability statement is given in the end of the manuscript.

Acknowledgements

The authors would like to thank Ms. Yang Fang for supporting the design of the figure of graphical abstract. Siming You acknowledges the Engineering and Physical Sciences Research Council (EPSRC) Programme Grant (EP/V030515/1) and Royal Society International Exchange Scheme (EC\NSFC\211175). This project was also partially funded by the European Union's Horizon 2020 research and innovation programme under the Marie Sklodowska-Curie grant agreement No. 101007976. All data supporting this study are provided in full in the paper.

References

[1] Fang Y, Paul MC, Varjani S, Li X, Park Y-K, You S. Concentrated solar thermochemical gasification of biomass: principles, applications, and development. Renew Sustain Energy Rev 2021;150:111484.
[2] Liu Q, Bai Z, Wang X, Lei J, Jin H. Investigation of thermodynamic performances for two solar-biomass hybrid combined cycle power generation systems. Energy Convers Manag 2016;122:252–62.
[3] El Alami K, Asbik M, Boualou R, Ouchani F-z, Agalit H, Rachidi S. A critical overview of the suitability of natural Moroccan rocks for high temperature thermal energy storage applications: towards an effective dispatching of concentrated solar power plants. J Energy Storage 2022;50:104295.
[4] Pramanik S, Ravikrishna R. A review of concentrated solar power hybrid technologies. Appl Therm Eng 2017;127:602–37.
[5] Puig-Arnavat M, Tora E, Bruno J, Coronas A. State of the art on reactor designs for solar gasification of carbonaceous feedstock. Sol Energy 2013;97:67–84.
[6] Chen J, Xu W, Zuo H, Wu X, J E, Wang T, et al. System development and environmental performance analysis of a solar-driven supercritical water gasification pilot plant for hydrogen production using life cycle assessment approach. Energy Convers Manag 2019;184:60–73.
[7] Ramachandran S, Yao Z, You S, Massier T, Stimming U, Wang C-H. Life cycle assessment of a sewage sludge and woody biomass co-gasification system. Energy 2017;137:369–76.
[8] Drost M, Antoniak Z, Brown D, Somasundaram S. Thermal energy storage for integrated gasification combined-cycle power plants. Richland, WA (USA): Pacific Northwest Lab.; 1990.
[9] Ansari SH, Ahmed A, Razzaq A, Hildebrandt D, Liu X, Park Y-K. Incorporation of solar-thermal energy into a gasification process to co-produce bio-fertilizer and power. Environ Pollut 2020;266:115103.
[10] Pinna-Hernández MG, Martínez-Soler I, Villanueva MJD, Fernández FGA, López JLC. Selection of biomass supply for a gasification process in a solar thermal hybrid plant for the production of electricity. Ind Crop Prod 2019;137:339–46.
[11] Kalaiselvam S, Parameshwaran R. Thermal energy storage technologies for sustainability: systems design, assessment and applications. Elsevier; 2014.
[12] Mahon H, O'Connor D, Friedrich D, Hughes B. A review of thermal energy storage technologies for seasonal loops. Energy 2022;239:122207.
[13] Nicotera I, Angjeli K, Coppola L, Enotiadis A, Pedicini R, Carbone A, et al. Composite polymer electrolyte membranes based on Mg–Al layered double hydroxide (LDH) platelets for H2/air-fed fuel cells. Solid State Ionics 2015;276: 40–6.
[14] Wang S, Zhang L, Liu C, Liu Z, Lan S, Li Q, et al. Techno-economic-environmental evaluation of a combined cooling heating and power system for gas turbine waste heat recovery. Energy 2021;231:120956.
[15] Kribus A, Zaibel R, Carey D, Segal A, Karni J. A solar-driven combined cycle power plant. Sol Energy 1998;62(2):121–9.
[16] Malato S, Maldonado MI, Fernandez-Ibanez P, Oller I, Polo I, Sánchez-Moreno R. Decontamination and disinfection of water by solar photocatalysis: the pilot plants of the Plataforma Solar de Almeria. Mater Sci Semicond Process 2016;42:15–23.
[17] Matsumura Y, Minowa T, Potic B, Kersten SR, Prins W, van Swaaij WP, et al. Biomass gasification in near-and super-critical water: status and prospects. Biomass Bioenergy 2005;29(4):269–92.
[18] Nakamura A, Kiyonaga E, Yamamura Y, Shimizu Y, Minowa T, Noda Y, et al. Detailed analysis of heat and mass balance for supercritical water gasification. J Chem Eng Jpn 2008;41(8):817–28.
[19] Boukis N, Galla U, Müller H, Dinjus E. Biomass gasification in supercritical water. Experimental progress achieved with the VERENA pilot plant. Conference Biomass gasification in supercritical water. Experimental progress achieved with the VERENA pilot plant. p. 1013.
[20] Yakaboylu O, Albrecht I, Harinck J, Smit K, Tsalidis G-A, Di Marcello M, et al. Supercritical water gasification of biomass in fluidized bed: first results and experiences obtained from TU Delft/Gensos semi-pilot scale setup. Biomass Bioenergy 2018;111:330–42.
[21] Chen J, Xu W, Zuo H, Wu X, Jiaqiang E, Wang T, et al. System development and environmental performance analysis of a solar-driven supercritical water gasification pilot plant for hydrogen production using life cycle assessment approach. Energy Convers Manag 2019;184:60–73.
[22] Kalinci Y, Hepbasli A, Dincer I. Life cycle assessment of hydrogen production from biomass gasification systems. Int J Hydrogen Energy 2012;37(19):14026–39.
[23] Powell KM, Rashid K, Ellingwood K, Tuttle J, Iverson BD. Hybrid concentrated solar thermal power systems: a review. Renew Sustain Energy Rev 2017;80: 215–37.
[24] Volkart K, Bauer C, Boulet C. Life cycle assessment of carbon capture and storage in power generation and industry in Europe. Int J Greenh Gas Control 2013;16: 91–106.
[25] Milani R, Szklo A, Hoffmann BS. Hybridization of concentrated solar power with biomass gasification in Brazil's semiarid region. Energy Convers Manag 2017;143: 522–37.
[26] Fthenakis V, Frischknecht R, Raugei M, Kim HC, Alsema E, Held M, et al. Methodology guidelines on life cycle assessment of photovoltaic electricity, vol. 12. IEA PVPS Task; 2011.
[27] Zhu X, Labianca C, He M, Luo Z, Wu C, You S, et al. Life-cycle assessment of pyrolysis processes for sustainable production of biochar from agro-residues. Bioresour Technol 2022:127601.
[28] Banacloche S, Herrera I, Lechón Y. Towards energy transition in Tunisia: sustainability assessment of a hybrid concentrated solar power and biomass plant. Sci Total Environ 2020;744:140729.
[29] Verghese KL, Horne R, Carre A. PIQET: the design and development of an online 'streamlined'LCA tool for sustainable packaging design decision support. Int J Life Cycle Assess 2010;15:608–20.
[30] Zhang Y, Baral A, Bakshi BR. Accounting for ecosystem services in life cycle assessment, part II: toward an ecologically based LCA. Environ Sci Technol 2010; 44(7):2624–31.
[31] Zhuang X, Xu X, Liu W, Xu W. LCOE analysis of tower concentrating solar power plants using different molten-salts for thermal energy storage in China. Energies 2019;12(7):1394.
[32] Gilani IH, Amjad M, Khan SS, Khan I, Larkin S, Raw B, et al. PEMFC application through coal gasification along with cost-benefit analysis: a case study for South Africa. Energy Explor Exploit 2021;39(5):1551–87.
[33] Koupaie EH, Leiva MB, Eskicioglu C, Dutil C. Mesophilic batch anaerobic co-digestion of fruit-juice industrial waste and municipal waste sludge: process and cost-benefit analysis. Bioresour Technol 2014;152:66–73.
[34] You S, Wang W, Dai Y, Tong YW, Wang C-H. Comparison of the co-gasification of sewage sludge and food wastes and cost-benefit analysis of gasification-and incineration-based waste treatment schemes. Bioresour Technol 2016;218: 595–605.
[35] Denholm P, Jorgenson J, Miller M, Zhou E, Wang C. Methods for analyzing the economic value of concentrating solar power with thermal energy storage. Golden, CO (United States): National Renewable Energy Lab.(NREL); 2015.
[36] Golberg A, Polikovsky M, Epstein M, Slegers PM, Drabik D, Kribus A. Hybrid solar-seaweed biorefinery for co-production of biochemicals, biofuels, electricity, and water: thermodynamics, life cycle assessment, and cost-benefit analysis. Energy Convers Manag 2021;246:114679.
[37] Fang Y, Ma L, Yao Z, Li W, You S. Process optimization of biomass gasification with a Monte Carlo approach and random forest algorithm. Energy Convers Manag 2022;264:115734.
[38] Hasnain S. Review on sustainable thermal energy storage technologies, Part I: heat storage materials and techniques. Energy Convers Manag 1998;39(11):1127–38.
[39] Abe T, Gokon N, Izawa T, Kodama T. Internally-circulating fluidized bed reactor using thermal storage material for solar coal coke gasification. Energy Proc 2015; 69:1722–30.
[40] Yang L, Zhang X, Liu S, Yu L, Zhang W. Field test of large-scale hydrogen manufacturing from underground coal gasification (UCG). Int J Hydrogen Energy 2008;33(4):1275–85.
[41] Aliaño-González MJ, Gabaston J, Ortiz-Somovilla V, Cantos-Villar E. Wood waste from fruit trees: biomolecules and their applications in agri-food industry. Biomolecules 2022;12(2):238.

[42] Cardoza D, Romero I, Martínez T, Ruiz E, Gallego FJ, López-Linares JC, et al. Location of biorefineries based on olive-derived biomass in Andalusia, Spain. Energies 2021;14(11):3052.
[43] Energy GR. Energy Yield And Performance Ratio Of Photovoltaic Systems. Green Rhino Energy. 2022.
[44] https://re.jrc.ec.europa.eu/pvg_tools/en/#TMY.[Access on 2023].
[45] Fernandez-Lopez M, López-González D, Puig-Gamero M, Valverde JL, Sanchez-Silva L. CO2 gasification of dairy and swine manure: a life cycle assessment approach. Renew Energy 2016;95:552–60.
[46] Llatas C. A model for quantifying construction waste in projects according to the European waste list. Waste Manag 2011;31(6):1261–76.
[47] Villoria Sáez P, del Río Merino M, Porras-Amores C. Estimation of construction and demolition waste volume generation in new residential buildings in Spain. Waste Manag Res 2012;30(2):137–46.
[48] Zamorano M, Molero E, Grindlay A, Rodríguez M, Hurtado A, Calvo F. A planning scenario for the application of geographical information systems in municipal waste collection: a case of Churriana de la Vega (Granada, Spain). Resour Conserv Recycl 2009;54(2):123–33.
[49] Arvanitoyannis IS. ISO 14040: life cycle assessment (LCA)–principles and guidelines. Waste Manag Food Indus 2008:97–132.
[50] Gupta R, Miller R, Sloan W, You S. Economic and environmental assessment of organic waste to biomethane conversion. Bioresour Technol 2022;345:126500.
[51] Zhou N, Zhou J, Dai L, Guo F, Wang Y, Li H, et al. Syngas production from biomass pyrolysis in a continuous microwave assisted pyrolysis system. Bioresour Technol 2020;314:123756.
[52] Wagner MJ, Wendelin T. SolarPILOT: a power tower solar field layout and characterization tool. Sol Energy 2018;171:185–96.
[53] Bhargav K, Gross F, Schramek P. Life Cycle cost optimized heliostat size for power towers. Energy Proc 2014;49:40–9.
[54] Pihl E. Reducing carbon emissions from natural gas-fired power plants. 2012.
[55] Piatkowski N, Wieckert C, Weimer AW, Steinfeld A. Solar-driven gasification of carbonaceous feedstock—a review. Energy Environ Sci 2011;4(1):73–82.
[56] Kuenlin A, Augsburger G, Gerber L, Maréchal F. Life cycle assessment and environomic optimization of concentrating solar thermal power plants. Conference Life cycle assessment and environomic optimization of concentrating solar thermal power plants.
[57] Singh B, Strømman AH, Hertwich E. Life cycle assessment of natural gas combined cycle power plant with post-combustion carbon capture, transport and storage. Int J Greenh Gas Control 2011;5(3):457–66.
[58] Gasa G, Lopez-Roman A, Prieto C, Cabeza LF. Life cycle assessment (LCA) of a concentrating solar power (CSP) plant in tower configuration with and without thermal energy storage (TES). Sustainability 2021;13(7):3672.
[59] Rubin ES, Chen C, Rao AB. Cost and performance of fossil fuel power plants with CO2 capture and storage. Energy Pol 2007;35(9):4444–54.
[60] Baratieri M, Baggio P, Bosio B, Grigiante M, Longo G. The use of biomass syngas in IC engines and CCGT plants: a comparative analysis. Appl Therm Eng 2009;29(16):3309–18.
[61] https://www.alibaba.com/product-detail/Hot-sale-auger-screw-conveyor-for_62166933656.html?spm=a2700.7724857.0.0.128279bbpq1HUB.[Access on 2023].
[62] Bauer C. Life cycle assessment of fossil and biomass power generation chains. An analysis carried out for ALSTOM Power Services. 2008.
[63] Verma A, Kumar A. Life cycle assessment of hydrogen production from underground coal gasification. Appl Energy 2015;147:556–68.
[64] Ouderji ZH, Gupta R, Mckeown A, Yu Z, Smith C, Sloan W, et al. Integration of anaerobic digestion with heat Pump: machine learning-based technical and environmental assessment. Bioresour Technol 2023;369:128485.
[65] Ascher S, Li W, You S. Life cycle assessment and net present worth analysis of a community-based food waste treatment system. Bioresour Technol 2020;305:123076.
[66] Jenkins S. The chemical engineering plant cost index.
[67] Turchi CS, Boyd M, Kesseli D, Kurup P, Mehos MS, Neises TW, et al. CSP systems analysis-final project report. Golden, CO (United States): National Renewable Energy Lab.(NREL); 2019.
[68] Kanniche M, Bouallou C. CO2 capture study in advanced integrated gasification combined cycle. Appl Therm Eng 2007;27(16):2693–702.
[69] Craig KR, Mann MK. Cost and performance analysis of biomass-based integrated gasification combined-cycle (BIGCC) power systems. Golden, CO (United States): National Renewable Energy Lab.(NREL); 1996.
[70] Descamps C, Bouallou C, Kanniche M. Efficiency of an integrated gasification combined cycle (IGCC) power plant including CO2 removal. Energy 2008;33(6):874–81.
[71] Cormos A-M, Cormos C-C. Techno-economic assessment of combined hydrogen & power co-generation with carbon capture: the case of coal gasification. Appl Therm Eng 2019;147:29–39.
[72] Mahajan K, Velaga NR, Kumar A, Choudhary A, Choudhary P. Effects of driver work-rest patterns, lifestyle and payment incentives on long-haul truck driver sleepiness. Transport Res F Traffic Psychol Behav 2019;60:366–82.
[73] Fuller JC, Schneider KP, Chassin D. Analysis of residential demand response and double-auction markets. Conference Analysis of residential demand response and double-auction markets. IEEE, p. 1-7.
[74] Gracia A, Barreiro-Hurlé J, y Pérez LP. Can renewable energy be financed with higher electricity prices? Evidence from a Spanish region. Energy Pol 2012;50:784–94.
[75] Solar T. Solar panels in Spain: facts. financing: tariffs, development; 2023.
[76] Zhang K, Wang Q, Liang Q-M, Chen H. A bibliometric analysis of research on carbon tax from 1989 to 2014. Renew Sustain Energy Rev 2016;58:297–310.
[77] Ortega-Izquierdo M, del Río P. Benefits and costs of renewable electricity in Europe. Renew Sustain Energy Rev 2016;61:372–83.
[78] IEA. Key energy statistics. 2020.
[79] Mann MK, Spath PL. Life cycle assessment of a biomass gasification combined-cycle power system. Golden, CO (United States): National Renewable Energy Lab. (NREL); 1997.
[80] Cohen GE, Kearney DW, Kolb GJ. Final report on the operation and maintenance improvement program for concentrating solar power plants. Albuquerque, NM, and Livermore, CA: Sandia National Laboratories (SNL); 1999.